Sensors and Actuators A 301 (2020) 111713

Contents lists available at ScienceDirect

Sensors and Actuators A: Physical

journal homepage: www.elsevier.com/locate/sna

Design, fabrication and experimental characterization of whole-thermoplastic microvalves and micropumps having micromilled liquid channels of rectangular and half-elliptical cross-sections

Amirhesam Banejad[a,b], Mohammad Passandideh-Fard[a], Hamidreza Niknam[a,b], Mohammad Javad Mirshojaeian Hosseini[b,c], Seyed Ali Mousavi Shaegh[b,d,*]

[a] Department of Mechanical Engineering, Ferdowsi University of Mashhad, Mashhad, Iran
[b] Orthopedic Research Center, Mashhad University of Medical Sciences, Mashhad, Iran
[c] School of Engineering Technology, Purdue Polytechnic Institute, 401 Grant St #150, West Lafayette, IN, 47907, USA
[d] Clinical Research Unit, Mashhad University of Medical Sciences, Mashhad, Iran

ARTICLE INFO

Article history:
Received 12 September 2019
Received in revised form 29 October 2019
Accepted 29 October 2019
Available online 21 November 2019

Keywords:
Thermoplastic materials
Micromilling
Microfluidic valves and pumps
Thermal bonding

ABSTRACT

Various designs and fabrication methods have been recently developed for the fabrication of whole-thermoplastic microfluidic actuators. In view of fabrication methods, micromilling has attracted attentions for high-precision micromachining of complex microfluidic structures. This method is also employed for cost-effective rapid prototyping of microdevices. In this study, the impacts of micromilled structures on the performance of gas-actuated microvalves and micropumps were reported. The liquid channels of the actuators were fabricated in rectangular and half-elliptical cross-sections in Poly(methyl methacrylate) PMMA to explore the geometrical effects on valving and pumping functions. Unlike the microvalve with rectangular cross-section, that of half-elliptical cross-section presented a leakage-free operation. Regarding the experimental characterization of micropumps, the maximum flow rates of 350.23 ± 6.13 and 382.50 ± 5.38 μl/min were obtained for the micropumps with rectangular and half-elliptical cross-sections, respectively. Compared to the rectangular cross-section, the half-elliptical one was more efficient in production of maximum flow rates at lower actuation gas pressures. However, fabricating rectangular micropump is more cost-effective in terms of required time and manpower. Thus, the appropriate channel design for micropump fabrication is determined by the final application of the pump, the operating conditions and the fabrication costs. Moreover, the robust performance of the actuators revealed that the presented method enables the production of microfluidic actuators for applications with long-term durability.

1. Introduction

Thermoplastics carry unique features that are very attractive for the fabrication of microfluidic devices [1]. Such motivation originates from high optical transparency [2,3], high cellular compatibility [4], low liquid evaporation through the compact polymeric structure [5], and high chemical resistance [6–8] of the thermoplastic materials. In addition, recyclability [9], cost-effectiveness [10], and compatibility with the existing manufacturing technologies for mass production [7,11] make thermoplastics as ideal materials for commercialized products. Various polymers such as cyclic olefin polymer (COP) [12–14], Poly methyl meta acrylate (PMMA)[15–17], cyclic olefin copolymer (COC) [18,19], poly styrene (PS) [20] and polycarbonate (PC) [21,22] have been employed in the literature to fabricate thermoplastic microfluidic components. However, the wide use of thermoplastics in research laboratories has been mainly hindered by the lack of access to proper rapid and cost-effective fabrication methods.

Fabrication methods such as injection molding [23], hot embossing [24], and thermoforming require pre-fabricated master molds to transfer patterns to thermoplastics. The fabrication of master molds for multi-layer microfluidic patterns, however, is costly and time-consuming [23,25,26]. In contrary, CO_2 laser micromachining and micromilling are considered as the most common

* Corresponding author.
E-mail address: Mousavisha@mums.ac.ir (S.A. Mousavi Shaegh).

https://doi.org/10.1016/j.sna.2019.111713
0924-4247/

methods to create patterns in thermoplastics without any need to use master molds. They require low start-up investment and provide rapid and cost-effective micromachining capabilities [27–37]. Owing to these features, different attempts have been directed towards the development of rapid prototyping methods for the fabrication of whole-thermoplastic microfluidics with embedded actuators [38–40].

Recently, Shaegh et al. [41] developed a fabrication method to produce whole-thermoplastic actuators such as microvalves and micropumps. They employed unfocused CO_2 laser ablation of PMMA to create curved liquid channel required for valve and pump fabrication using Quake's design. The engraved channels were treated with chloroform to remove the micro cavities formed by the decomposition and evaporation of PMMA induced by the CO_2 laser beam.

Compared to the CO_2 laser micromachining, the micromilling method has been less reported for the fabrication of whole-thermoplastic actuators [42]. The micromilling is a subtractive fabrication method in which a rotating cutting tool is utilized to remove material from a starting stock piece. This method provides a higher precision for the fabrication of microstructures in thermoplastics compared to the CO_2 laser micromachining method. Engraved patterns through the use of CO_2 laser micromachining have generally near-Gaussian geometries [43]. The micromilling method, however, enables the fabrication of a wide range of complex geometries including undercuts, rounded surfaces, and sharp internal corners [42]. In this way, micromilling method allows for the creation of various microfluidic functional elements in desired geometries. Thus, the geometry of the components could be modulated for optimum operation in various applications.

In this study, the effect of liquid channel geometry on the operation of gas-actuated microvalves and micropumps was investigated (Fig. 1). To this end, optimized micromilling process was employed to create liquid channels with rectangular and half-elliptical geometries in PMMA (Fig. 2). The fabrication process enabled the creation of liquid channels with low surface roughness while no further physical and chemical treatment were used to enhance the surface quality. The multilayer whole-thermoplastic actuators were achieved using thermal fusion bonding method, while TPU film was employed as an actuation membrane. Two designs of microvalves along with two designs of micropumps having rectangular and half-elliptical liquid cross-sections were fabricated and characterized. Results revealed that the half-elleptical cross-section is desired for leakage-free valve operation, while the micropump with rectangular cross-section could be also employed for pumping purposes with satisfactory operation.

2. Experimental Setup

2.1. Materials and apparatus

Commercially-available cast acrylic (also known as PMMA) sheets (Calvin, Vietnam) in thicknesses of 1 and 2 mm were used as the structural materials for the fabrication of microvalves and micropumps components. A commercial CNC micromilling (DSP, China), with a worktable (X and Y-axis) and an adjustable spindle in X, Y and Z axes, was used for the micromachining of PMMA sheets. The liquid channels were drilled using a two-flute, square-end mill (also known as a flat end mill) with a diameter of 0.3 mm, a spindle speed of 22000 rpm and different feed rates of 75 and 90 mm/min. The work features were prepared using the SOLIDWORKS® software (Version 2016) to create computer-aided design (CAD) files. The Mastercam® software (Version 2017) was employed to convert the CAD files into a series of G-codes for running the micromilling machine. The TPU film (PT9200US NAT 1.0 mil, Covestro LLC, MA, USA) with a thickness of 25 μm was used as a membrane for actuation purposes. The TPU film is widely employed in biomedical applications owing to its unique features including biocompatibility, resilient mechanical properties, and hyper elasticity [44–47]. A conventional laboratory vacuum oven (AFE200LV-60DH, ATRA, IRAN) was used for the thermal treatment and bonding of PMMA sheets and the TPU film. To activate the gas-actuated microfluidic devices in desired frequencies, pneumatic fast switches (FESTO®, MH1-24 V DC) synchronized with a controller system (WAGO®, Fieldbus controller, System 750) were employed. The controller was interfaced with a PC through a program developed in the CODESYS® software. Nitrogen gas supplied from a cylinder was used for actuation purposes. The Tygon® tubing was used to connect the solenoid valves to fabricated chips. The gas pressure was adjusted using two pressure regulators within a range of 8 kPa to more than 300 kPa. For the flow visualization, deionized water was mixed with red food dye with a volume ratio of 200:1.

2.2. Design and fabrication of the thermoplastic components

The structure of the normally open, multilayer, pneumatic-actuated microvalve included a control chamber, a liquid channel and a diaphragm. The flow control could be achieved through the TPU film deflection by regulating the gas pressure (Fig. 1a and b). The peristaltic micropumps were developed using five interconnected microvalves in series (Fig. 1c and d). Various flow rates could be produced through the consecutive actuation of the microvalves in desired patterns presented later in this paper. Important dimensions of microdevices were shown in Fig. 1e and f. The diameters of circulars holes, the length of liquid channel and the length of gas channel were designed to be 1.6 mm, 40 mm and 8.88 mm, respectively.

The liquid channel of the micropumps was created in two cross-sections of rectangular and half-elliptical geometries with similar flow areas and channel heights. In this way, the height of 0.15 mm was opted for both designs, and the width of half-elliptical and rectangular micropump were 1.237 and 0.97 mm, respectively. The multilayer actuators were initially designed in the SOLIDWORKS® and post-processed with the Mastercam® for the subsequent machining. The microstructures were created in the PMMA sheets using the micromilling machine while the TPU layer was cut in desired dimensions using a CO_2 laser machine or a blade (Fig. 2).

The micromachined components were inspected using a field emission scanning electron microscope (FESEM) (TESCAN, MIRA3) (Fig. 3a-d). Furthermore, the surface roughness of the micromachined liquid channels was investigated using an atomic force microscope (AFM). As shown in Fig. 3e, smooth surfaces were obtained through the use of a proper feed rate and spindle velocity, as they have considerable effects on the surface quality [42,48]. To investigate the surface roughness, parameters including average roughness (Ra), RMS roughness (Rq) and Peak-to-Valley roughness (Rz) were evaluated. In this way, the corresponding surface roughness parameters were measured as Ra=15.70 nm, Rq=23.67 nm, Rz=259.20 nm for the channels with half-elliptical cross-section and Ra=14.98 nm, Rq=19.31 nm, Rz=142.3 nm for the channels with rectangular cross-section, which are appropriate for microfluidic applications [49].

The thermal fusion bonding was employed to bond the fabricated layers. The procedure of this bonding method relies on matching the glass transition temperature of the employed thermoplastics. To obtain high quality bonding surfaces with a minimum deformation and bubble entrapment between the layers, the bonding temperature, pressure, and time were controlled precisely [50]. To start with, all PMMA components were washed using a conventional laboratory detergent and ethanol solution.

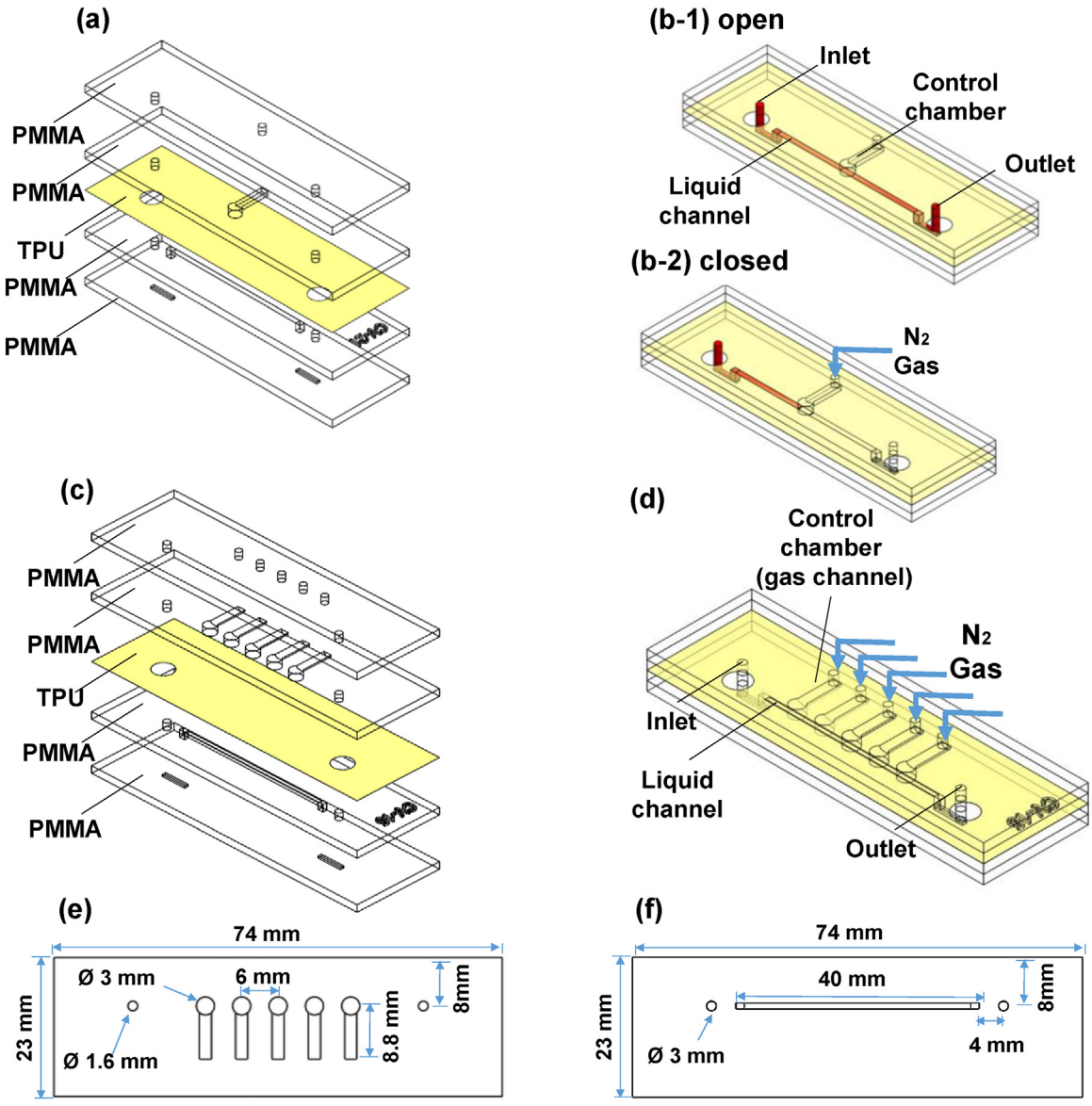

Fig. 1. Design of the microdevices. (a) Exploded view for the multi-layer microvalve; (b) schematics for the operation of the microvalves; (c) exploded view for the multi-layer microvalve; (d) schematics for the operation of the micropumps; (e) the dimensions of the layer having control chamber; (e) the dimensions of the layer having liquid channel.

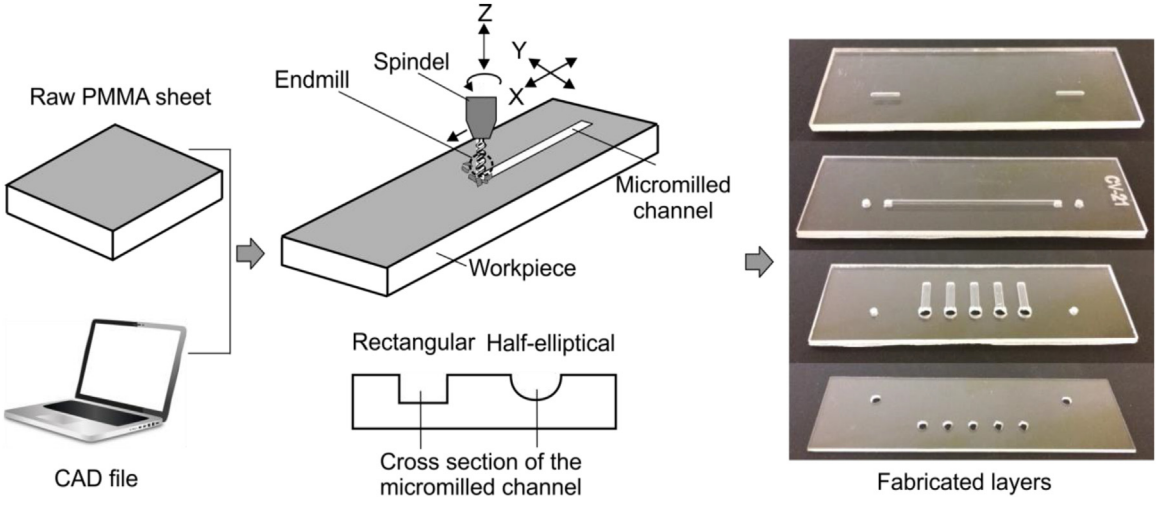

Fig. 2. Schematic illustration of the fabrication process.

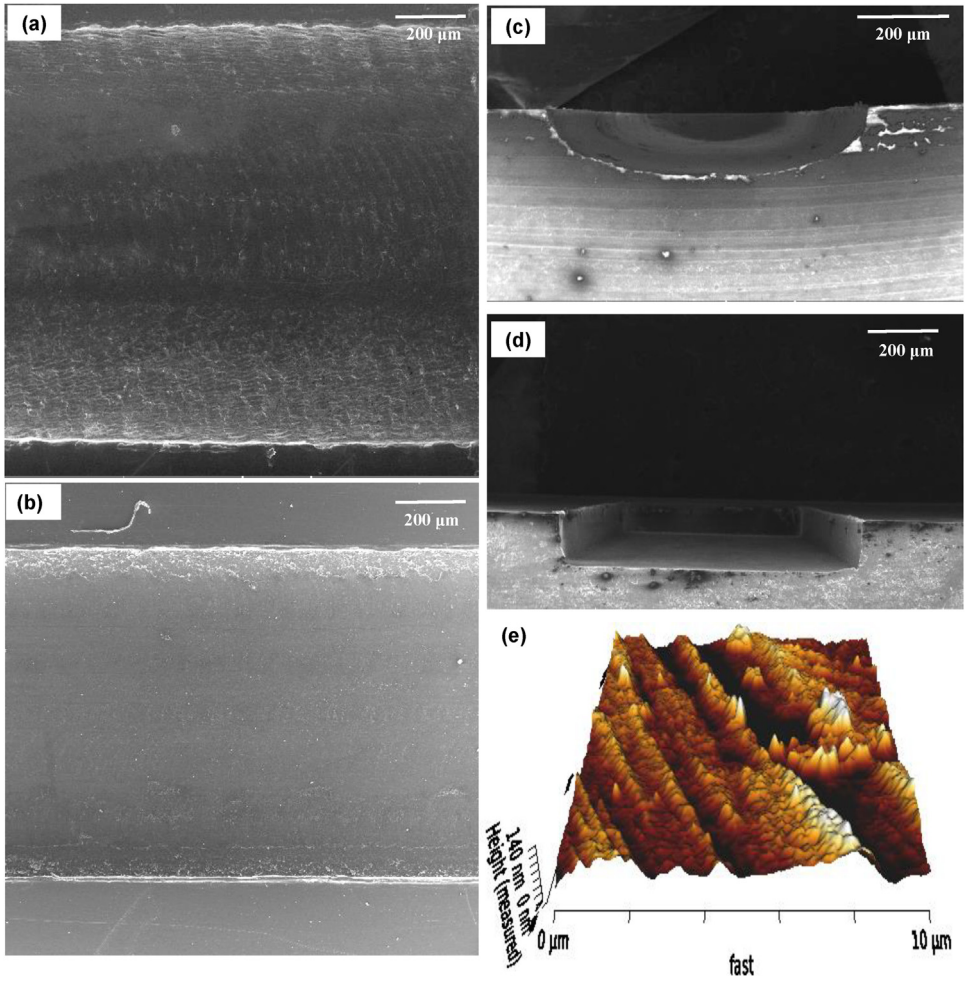

Fig. 3. Field emission scanning electron microscope (FESEM) and atomic force microscopic (AFM) images of the fabricated channels. (a) FESEM image of the half-elliptical channel; (b) FESEM image of the rectangular channel; (c) FESEM image of the half-elliptical cross-section; (d) FESEM image of the rectangular cross-section; (e) AFM image of a fabricated channel.

Then, the layers were thermally treated in the vacuum oven at a temperature of 90 °C and a pressure (gauge pressure) of −80 kPa for at least 8 hours with a subsequent gradual cooling to the room temperature. This step is necessary to release the dissolved gases entrapped within the bulk PMMA specimens [41]. In the next step, the PMMA layers and the TPU membrane were aligned and sandwiched between two glass slides using two paper clips with a width of 30 mm. Afterwards, the assembly was treated at 140 °C and −80 kPa for 60 minutes followed by a gradual cooling process to the room temperature in 50 minutes. It should be noted that the glass transition temperature (T_g) of commercial PMMA lies in the range of 85 °C – 165 °C [51]. This originates from the large number of commercially-available compositions which are copolymers/commoners compared to methyl meta acrylate [51].

2.3. Experiments for the microvalve characterization

Fig. 4a shows the experimental setup to characterize the fabricated microvalve. The test setup consisted of a liquid reservoir, a nitrogen gas tank, a controller system, a pneumatic solenoid valve, two gas regulators and the interconnecting tubing. The liquid reservoir was pressurized with nitrogen gas in desired pressures to create various liquid flow rates through the microvalve for the leakage test. The pressure of the reservoir could be adjusted by using the pressure regulator (Fig. 4a, **regulator 1**). The valve actuation was performed using a custom-made controller system consisting of a pneumatic solenoid valve in which its operation could be modulated by a programmable WAGO® controller. The CODESYS® software was employed to create a custom-made interface program for command communication between the solenoid valve and the controller. The Tygon® tubing was used to connect the solenoid valves to the control chamber of the microvalve. A precise gas regulator (Fig. 4a, **regulator 2**) was used to adjust the actuation gas pressure. Finally, the leakage flow rate through the microvalve was calculated by measuring the length of the liquid column in the Tygon® tube in a certain time period. The inner diameter of the Tygon® tube was 0.020 inch.

2.4. Experiments for the micropump characterization

The micropump characterization setup was similar to that of the microvalve. The only difference was associated with the liquid reservoir having an atmospheric pressure (Fig. 4b). The fabricated peristaltic micropump consisted of five serial interconnected microvalves for pumping liquid by consecutive actuation. The actuation of the microvalves in desired frequencies was obtained using five solenoid valves controlled by the WAGO® controller. Similar

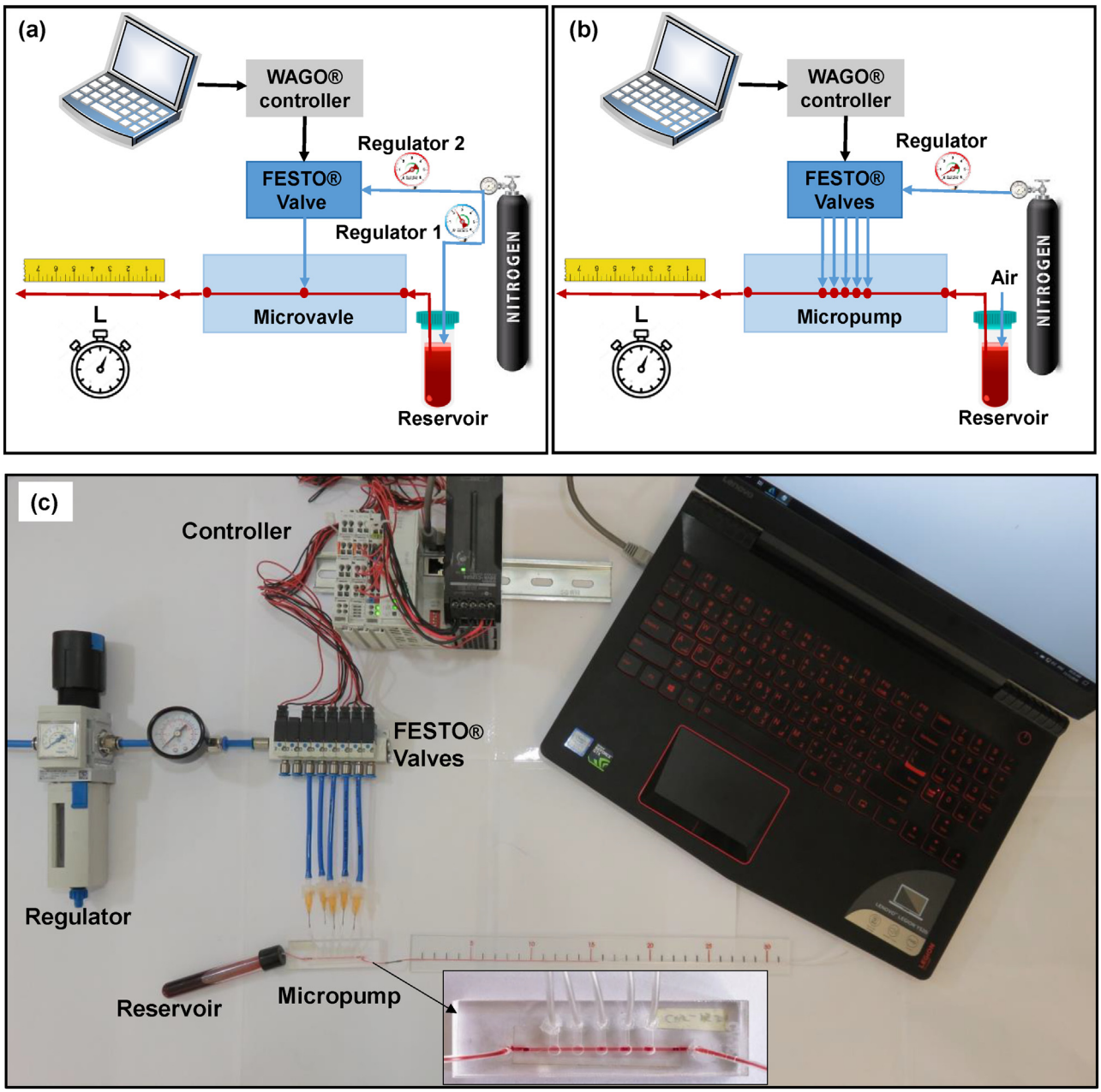

Fig. 4. (a) Schematic illustration of the microvalve performance test; (b) schematic illustration of the microvalve performance test; (c) image of the experimental setup.

to microvalve actuation, a custom-made CODESYS® program was developed to regulate the actuation frequencies (Fig. 4b and c).

3. Results and Discussions

3.1. The characterization of microvalves

Initially, the bonding strength of the fabricated microvalves was tested. To this end, nitrogen gas with pressures up to 700 kPa was applied in the control chamber once the entire microvalve was immersed in water. No bubble and burst failure was observed. In addition, a water-based liquid, containing a red dye, with pressures up to 300 kPa was introduced in the liquid channel while the outlet of the microvalve was blocked. No leakage from the bonded layers was observed.

Fig. 5 demonstrates the microvalve volume flow rate versus actuation gas pressures for the designs of microvalve consisting of liquid channels with half-elliptical cross-section. The valve with the liquid pressures of 8 and 18 kPa generated flow rates of about 1.5 and 2.5 ml/min, respectively. In general, the liquid flow rate decreased once the pressure of gas for valve actuation was increased. As shown in Fig. 5, for the half-elliptical microvalve with a liquid pressure of 8 kPa and an actuation gas pressure of 140 kPa, the leakage flow rate had a negligible value of 0.08 μl/min. When the liquid pressure was increased to 18 kPa and actuation gas pressure 220 kPa, the leakage value was only 0.15 μl/min. In the other hand, the microvalve with rectangular cross-section could not achieve a leakage-free operation. Based on the fact that the basis of these normally-open microvalves is on the membrane coverage of the liquid channel, the channel with rectangular cross-section having straight corners, could not be employed for valving purposes. By contrast, the shape of the half-elliptical cross-section can provide a uniform and smooth valve seat for the deformed TPU membrane that has a curved deflection profile.

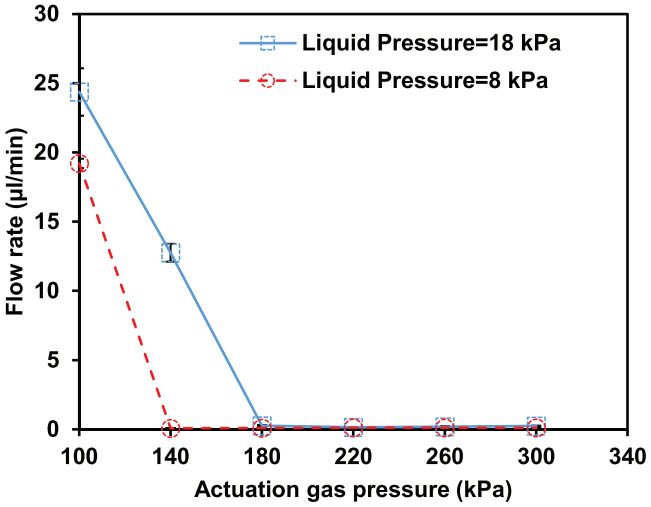

Fig. 5. Leakage rate vs. actuation gas pressure for the half-elliptical microvalve.

3.2. The characterization of micropumps

The two fabricated micropumps having rectangular and half-elliptical liquid channels consisted of five serial interconnected microvalves with consecutive operation at predefined frequencies (Fig. 6a). A custom-made program was developed to control the operation of the pneumatic valves at a predefined frequency pattern (Fig. 6b) **(Video S1)**.

Fig. 6c and d demonstrate the effect of varying actuation frequency on the pumping flow rate at four actuation pressures of 50, 100, 160, and 220 kPa for both pump designs. Overall, the increase of actuation frequency enhanced the pumping flow rate. However, an optimum actuation pressure, that produced the maximum flow rate, was obtained for both pumps. The maximum flow rates of 382.497 ± 5.38 µl/min for the half-elliptical pump design and 350.23 ± 6.13 µl/min for the rectangular pump design were obtained at gas actuation pressures of 100 and 160 kPa, respectively. The higher generated flow rate of the micropump with half-elliptical channel could be associated with a better membrane coverage over the curve surface. Therefore, the half-elliptical cross-section could produce an appropriate valve seat with minimal liquid leakage during actuation. Compared to the rectangular liquid channel, the approximate blockage of the liquid in the half-elliptical cross-section could be achieved at lower gas pressures. Furthermore, the micropumps with half-elliptical and rectangular cross-section had optimum gas pressures of 100 kPa and 160 kPa, respectively, for which the generated flow rate were maximum. It means that as the amount of gas actuation pressure is more than that of optimum one, the oscillation amplitude of membrane is reduced leading to reduction of generated flow rate.

The effect of downstream pressure, i.e. liquid backpressure, on the generated flow rate was shown in Fig. 6e and f. A liquid column with an adjustable height was implemented at the outlet port of the fabricated micropump, while the inlet port of the pump was linked to a reservoir of food dye-water solution maintained at the atmospheric pressure. The downstream pressure was altered by varying the height of the liquid column (H). Experiments were performed using actuation gas pressures of 100 and 200 kPa at a frequency of 5 Hz. As shown in Fig. 6e, at an actuation gas pressure of 200 kPa, the pumping flow rate was decreased from 196.5 ± 9 µl/min to 17.50 ± 1 µl/min once the downstream pressure was increased from nearly 0.2 kPa (20-mm liquid column) to about 1.4 kPa (140-mm liquid column). The pumping flow rate of the micropump with the half-elliptical liquid channel was decreased from 118.57 ± 3.9 µl/min to 8.85 ± 0.5 µl/min as the downstream pressure was increased from about 0.4 kPa (40-mm liquid column) to approximately 3 kPa (300-mm liquid column) (Fig. 6f).

To compare the operation of micropumps, the ratio of generated flow rate of half-elliptical micropump to that of rectangular one was shown as a function of gas actuation pressure for four gas actuation frequencies of 1, 5, 10, and 15 Hz (Fig. 7a). It is clear that for all frequencies, as the applied gas pressure rose, this ratio declined consistently. Consequently, compared to half-elliptical micropump, increasing the applied gas pressure resulted in that the rectangular one was considered a more efficient candidate in terms of generated flow rate to be implemented in microfluidic devices.

To investigate the durability of fabricated micropumps, the long-term operation of the fabricated micropump with the rectangular cross-section was examined for more than one million actuation cycles. The micropump could continuously generate a stable flow rate ranged from 85.7 µl/min to 93.1 µl/min using an actuation gas pressure of 100 kPa (Fig. 7b). The minor fluctuations of the measured flow rate could be due to slight changes in the actuation gas pressure. Due to the high durability of the micropump, it could be utilized for a wide range of on-chip purposes such as drug testing and microfluidic cell cultures in which the liquid pumping is necessary for an extended period of time.

In addition to the performance of fabricated micropumps, some factors such as fabrication time and cost could be investigated. In this way, the time needed for fabricating rectangular channel is approximately twice more than that of half-elliptical one. Therefore, compared to half-elliptical geometry, using rectangular one is more efficient in terms of time and manpower.

4. Conclusion

This article reported on the development of whole-thermoplastic microfluidic microvalves and micropumps using commercially available PMMA sheet, and TPU film. The liquid channels of the actuators were fabricated in two cross-sections of half-elliptical and rectangular geometries. The high-precision micromilling was employed to make microstructures in cast PMMA sheets, and the TPU film was used as a stretchable membrane to achieve flow manipulations required for gas-actuated valving/pumping purposes. The AFM characterizations revealed that the developed micromilling process allowed for the production of highly smooth surfaces in channels with half-elliptical and rectangular cross-sections. Compared to CO_2 laser micromachining, micromilling method enables the fabrication of a wide spectrum of geometries with high surface quality eliminating post-fabrication surface treatments. The production of high strength multilayer microvalves and micropumps was achieved through the low-pressure thermal fusion bonding of the components with no physical or chemical surface treatment. The microvalve with half-elliptical cross-section presented a leakage-free operation that is suitable for on-chip flow manipulations. In addition, at a same frequency, the micropump with half-elliptical cross-section needed a lower actuation pressure to generate a desired flow rate compared to the micropump with rectangular cross-section. Thus, full coverage of the liquid channel was not necessary for the operation of micropump. However, this cross-section may result in larger back flow and lower pumping flow rate. Regarding fabrication features, required time for the micromilling of the liquid channel with half-elliptical cross-section was more than twice of the required time for the fabrication of rectangular cross-section. In this way, the geometrical design of the pump could be determined based on its application and operation features such as accessible actuation pressure and required liquid pressure at

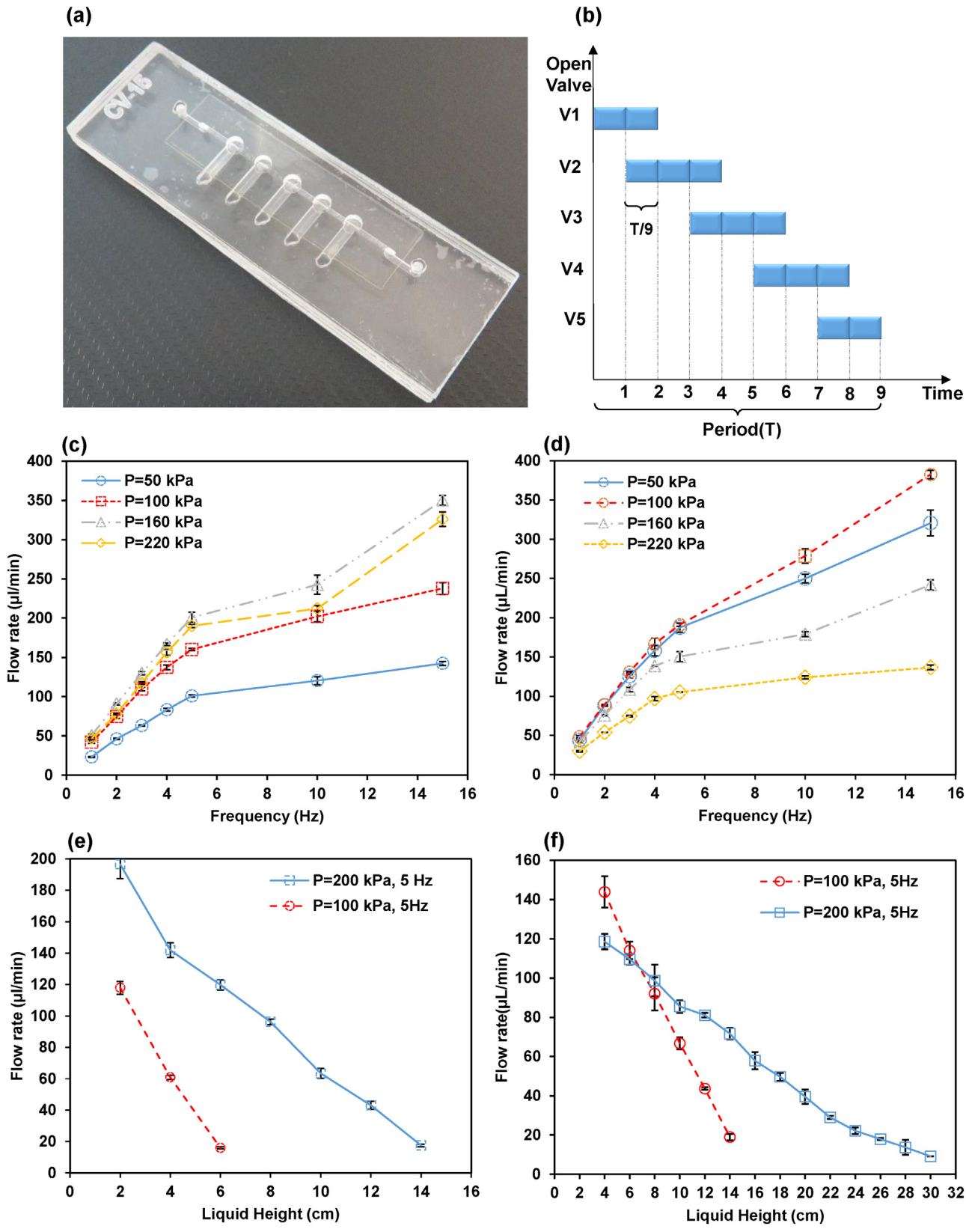

Fig. 6. Fabrication, performance and characterization of the micropumps. (a) The image of a fabricated micropump; (b) micropump actuation pattern; (c) the effect of actuation gas pressure and the frequency of actuation on pumping flow rate in micropump with rectangular cross-section; (d) the effect of actuation pressure and the frequency of actuation on pumping flow rate in micropump with half-elliptical cross-section; (e) the effect of backpressure on pumping flow rate in the rectangular micropump; pressure difference between the inlet and the outlet ports of the micropump was produced through increasing the height of the outlet port; (f) the effect of backpressure on pumping flow rate in the half-elliptical micropump.

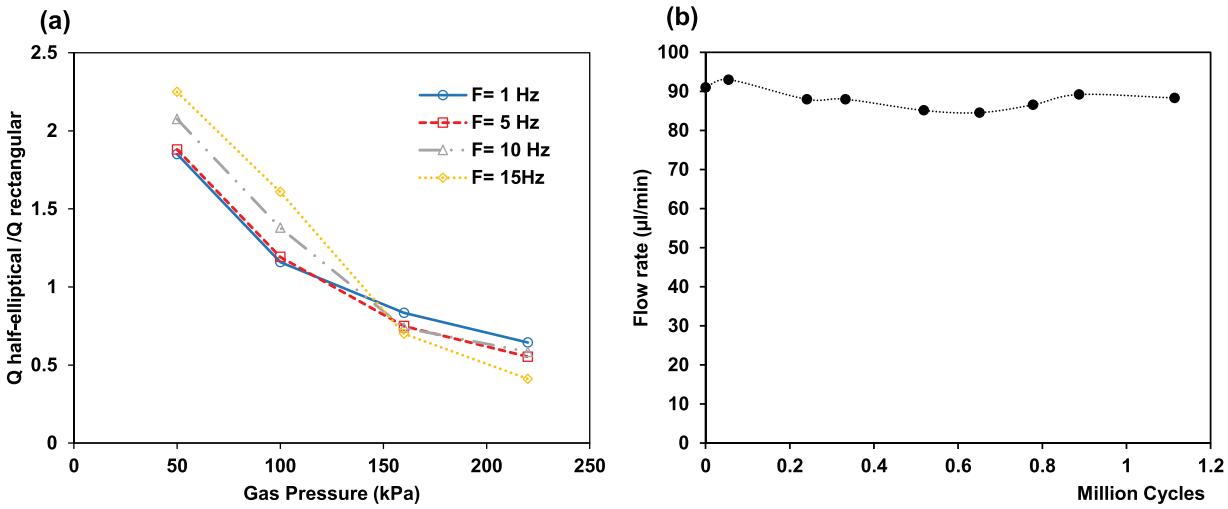

Fig. 7. (a) The effect of gas actuation pressure on the ratio of generated flow rate of half-elliptical micropump to that of rectangular micropump; (b) Long-term performance of the micropump with rectangular cross-section for liquid pumping for more than one million cycles (four days); the frequency of actuation was 3 Hz with an actuation air pressure of 100 kPa; error bars for recorded data points were ±5% of the average of each point.

the pump outlet. For commercialization considerations, the overall fabrication costs, including manpower and cutting tool expenses, also play critical roles on the proper geometrical design of an actuator. In overall, the micropump could present a flawless and robust long-term performance for more than one million actuation cycles. Owing to the unique features of the fabricated actuators, the proposed fabrication process enables the rapid production of high-performance whole-thermoplastic microfluidic actuators for research labs as well as for commercialized applications. To this end, the presented actuators could be widely employed for various on-chip applications including pumping a flow manipulation, micromixing [52], and liquid dispensing and droplet generation [53].

Acknowledgment

S. A. M. S. gratefully acknowledges funding by National Institute for Medical Research Development (NIMAD) under grant number 957144.

Appendix A. Supplementary data

Supplementary material related to this article can be found, in the online version, at doi:https://doi.org/10.1016/j.sna.2019.111713.

References

[1] N.-T. Nguyen, S.T. Wereley, S.A.M. Shaegh, Fundamentals and applications of microfluidics, Third ed., ed., Artech house, 2019.
[2] H. Becker, L.E. Locascio, Polymer microfluidic devices, Talanta. 56 (2002) 267–287, http://dx.doi.org/10.1016/S0039-9140(01)00594-X.
[3] G. Khanarian, Optical properties of cyclic olefin copolymers, Optical Engineering. 40 (2001) 1024–1030, http://dx.doi.org/10.1117/1.1369411.
[4] E. Berthier, E.W. Young, D. Beebe, Engineers are from PDMS-land, Biologists are from Polystyrenia, Lab on a Chip. 12 (2012) 1224–1237, http://dx.doi.org/10.1039/C2LC20982A.
[5] C.J. Ochs, J. Kasuya, A. Pavesi, R.D. Kamm, Oxygen levels in thermoplastic microfluidic devices during cell culture, Lab on a Chip. 14 (2014) 459–462, http://dx.doi.org/10.1039/C3LC51160J.
[6] D. Voicu, G. Lestari, Y. Wang, M. DeBono, M. Seo, S. Cho, E. Kumacheva, Thermoplastic microfluidic devices for targeted chemical and biological applications, RSC Advances. 7 (2017) 2884–2889, http://dx.doi.org/10.1039/C6RA27592C.
[7] E.K. Sackmann, A.L. Fulton, D.J. Beebe, The present and future role of microfluidics in biomedical research, Nature. 507 (2014) 181–190, http://dx.doi.org/10.1038/nature13118.
[8] K.M. Weerakoon-Ratnayake, C.E. O'Neil, F.I. Uba, S.A. Soper, Thermoplastic nanofluidic devices for biomedical applications, Lab on a Chip. 17 (2017) 362–381, http://dx.doi.org/10.1039/C6LC01173J.
[9] A.M. Wan, D. Devadas, E.W. Young, Recycled polymethylmethacrylate (PMMA) microfluidic devices, Sensors and Actuators B: Chemical. 253 (2017) 738–744, http://dx.doi.org/10.1016/j.snb.2017.07.011.
[10] C.-W. Tsao, Polymer Microfluidics: Simple, Low-Cost Fabrication Process Bridging Academic Lab Research to Commercialized Production, Micromachines. 7 (2016) 225–236, http://dx.doi.org/10.3390/mi7120225.
[11] K. Liu, Z.H. Fan, Thermoplastic microfluidic devices and their applications in protein and DNA analysis, Analyst. 136 (2011) 1288–1297, http://dx.doi.org/10.1039/C0AN00969E.
[12] C.D. Chin, V. Linder, S.K. Sia, Commercialization of microfluidic point-of-care diagnostic devices, Lab on a Chip. 12 (2012) 2118–2134, http://dx.doi.org/10.1039/C2LC21204H.
[13] A.O.S. Ali Aghvamia, Z.K. Zhangb, Markus Ludwiga, Michael Heymanna, Michael Nortona, Niya Wilkinse, Seth Fradena, Rapid prototypal of cyclic olefin copolymer (COC) microfluidic devices, Sensors and Actuators B: Chemical. 247 (2017) 940–949, http://dx.doi.org/10.1016/j.snb.2017.03.023.
[14] D. Konstantinou, A. Shirazi, A. Sadri, E.W. Young, Combined hot embossing and milling for medium volume production of thermoplastic microfluidic devices, Sensors and Actuators B: Chemical. 234 (2016) 209–221, http://dx.doi.org/10.1016/j.snb.2016.04.147.
[15] K.T.L. Trinh, Q.N. Pham, N.Y. Lee, Clog-free and reliable solvent bonding of poly (methyl methacrylate) microdevice mediated by eco-friendly acetic acid at room temperature and its application for polymerase chain reaction and human cell culture, Sensors and Actuators B: Chemical. 282 (2019) 1008–1117, http://dx.doi.org/10.1016/j.snb.2018.10.077.
[16] C. Matellan, E. Armando, Cost-effective rapid prototyping and assembly of poly (methyl methacrylate) microfluidic devices, Scientific reports. 8 (2018) 6971–6985, http://dx.doi.org/10.1038/s41598-018-25202-4.
[17] Y. Chen, L. Zhang, G. Chen, Fabrication, modification, and application of poly (methyl methacrylate) microfluidic chips, Electrophoresis. 29 (2008) 1801–1814, http://dx.doi.org/10.1002/elps.200700552.
[18] O.D. Rahmanian, D.L. DeVoe, Single-use thermoplastic microfluidic burst valves enabling on-chip reagent storage, Microfluidics and nanofluidics. 18 (2015) 1045–1053, http://dx.doi.org/10.1007/s10404-014-1494-8.
[19] S. Wouters, J. De Vos, J.L. Dores-Sousa, B. Wouters, G. Desmet, S. Eeltink, Prototyping of thermoplastic microfluidic chips and their application in high-performance liquid chromatography separations of small molecules, Journal of Chromatography A. 1523 (2017) 224–233, http://dx.doi.org/10.1016/j.chroma.2017.05.063.
[20] S. Puza, E. Gencturk, I.E. Odabasi, E. Iseri, S. Mutlu, K.O. Ulgen, Fabrication of cyclo olefin polymer microfluidic devices for trapping and culturing of yeast cells, Biomedical microdevices. 19 (2017) 40, http://dx.doi.org/10.1007/s10544-017-0182-3.
[21] K.S. Lee, R.J. Ram, Plastic–PDMS bonding for high pressure hydrolytically stable active microfluidics, Lab on a Chip. 9 (2009) 1618–1624, http://dx.doi.org/10.1039/B820924C.
[22] Y. Fan, S. Liu, J. He, K. Gao, Y. Zhang, Rapid and low-cost hot-embossing of polycaprolactone microfluidic devices, Materials Research Express. 5 (2018), 015305, http://dx.doi.org/10.1088/2053-1591/aaa3bc.
[23] J. Giboz, T. Copponnex, P. Mélé, Microinjection molding of thermoplastic polymers: a review, Journal of micromechanics and microengineering. 17 (2007) 96–109, http://dx.doi.org/10.1088/0960-1317/17/6/R02.

[24] S. Yang, D.L. DeVoe, Microfluidic device fabrication by thermoplastic hot-embossing, Microfluidic Diagnostics: Methods and Protocols (2013) 115–123, http://dx.doi.org/10.1007/978-1-62703-134-9_8.
[25] H. Becker, C. Gärtner, Polymer microfabrication technologies for microfluidic systems, Analytical and bioanalytical chemistry. 390 (2008) 89–111, http://dx.doi.org/10.1007/s00216-007-1692-2.
[26] H. Becker, C. Gärtner, Polymer microfabrication methods for microfluidic analytical applications, ELECTROPHORESIS: An International Journal. 21 (2000) 12–26, http://dx.doi.org/10.1002/(SICI)1522-2683(20000101)21:1<12::AID-ELPS12>3.0.CO;2-7.
[27] Z. Strike, K. Ghofrani, C. Backhouse, CO2 Laser-Based Rapid Prototyping of Micropumps, Micromachines. 9 (2018) 215–224, http://dx.doi.org/10.3390/mi9050215.
[28] L. Gu, G. Yu, C.-W. Li, A fast and low-cost microfabrication approach for six types of thermoplastic substrates with reduced feature size and minimized bulges using sacrificial layer assisted laser engraving, Analytica chimica acta. 997 (2018) 24–34, http://dx.doi.org/10.1016/j.aca.2017.10.030.
[29] O. Cybulski, S. Jakiela, P. Garstecki, Whole Teflon valves for handling droplets, Lab on a Chip. 16 (2016) 2198–2210, http://dx.doi.org/10.1039/C6LC00375C.
[30] E.F.M. Gabriel, W.K.T. Coltro, C.D. Garcia, Fast and versatile fabrication of PMMA microchip electrophoretic devices by laser engraving, Electrophoresis. 35 (2014) 2325–2332, http://dx.doi.org/10.1002/elps.201300511.
[31] C. Chung, S. Lin, On the fabrication of minimizing bulges and reducing the feature dimensions of microchannels using novel CO2 laser micromachining, Journal of Micromechanics and Microengineering. 21 (2011), 065023, http://dx.doi.org/10.1088/0960-1317/21/6/065023.
[32] S. Liu, Y. Fan, K. Gao, Y. Zhang, Fabrication of Cyclo-olefin polymer-based microfluidic devices using CO2 laser ablation, Materials Research Express. 5 (2018), 095305, http://dx.doi.org/10.1088/2053-1591/aad72e.
[33] T.-F. Hong, W.-J. Ju, M.-C. Wu, C.-H. Tai, C.-H. Tsai, L.-M. Fu, Rapid prototyping of PMMA microfluidic chips utilizing a CO 2 laser, Microfluidics and nanofluidics. 9 (2010) 1125–1133, http://dx.doi.org/10.1007/s10404-010-0633-0.
[34] K. Liu, J. Xiang, Z. Ai, S. Zhang, Y. Fang, T. Chen, Q. Zhou, S. Li, S. Wang, N. Zhang, PMMA microfluidic chip fabrication using laser ablation and low temperature bonding with OCA film and LOCA, Microsystem Technologies. 23 (2017) 1937–1942, http://dx.doi.org/10.1007/s00542-016-2924-1.
[35] S. Prakash, S. Kumar, Fabrication of microchannels on transparent PMMA using CO 2 Laser (10.6 μm) for microfluidic applications: An experimental investigation, International Journal of Precision Engineering and Manufacturing. 16 (2015) 361–366, http://dx.doi.org/10.1002/10.1007/s12541-015-0047-8.
[36] S. Prakash, S. Kumar, Experimental and theoretical analysis of defocused CO2 laser microchanneling on PMMA for enhanced surface finish, Journal of Micromechanics and Microengineering. 27 (2016), 025003, http://dx.doi.org/10.1088/1361-6439/27/2/025003.
[37] H. Qi, X. Wang, T. Chen, X. Ma, T. Zuo, Fabrication and characterization of a polymethyl methacrylate continuous-flow PCR microfluidic chip using CO 2 laser ablation, Microsystem technologies. 15 (2009) 1027–1030, http://dx.doi.org/10.1007/s00542-009-0843-0.
[38] S.A.M. Shaegh, Z. Wang, S.H. Ng, R. Wu, H.T. Nguyen, L.C.Z. Chan, A.G.G. Toh, Z. Wang, Plug-and-play microvalve and micropump for rapid integration with microfluidic chips, Microfluidics and Nanofluidics. 19 (2015) 557–564, http://dx.doi.org/10.1007/s10404-015-1582-4.
[39] K. Ren, W. Dai, J. Zhou, J. Su, H. Wu, Whole-Teflon microfluidic chips, Proceedings of the National Academy of Sciences 108 (2011) 8162–8166, http://dx.doi.org/10.1073/pnas.1100356108.
[40] A. Pourmand, S.A.M. Shaegh, H.B. Ghavifekr, E.N. Aghdam, M.R. Dokmeci, A. Khademhosseini, Y.S. Zhang, Fabrication of whole-thermoplastic normally closed microvalve, micro check valve, and micropump, Sensors and Actuators B: Chemical. 262 (2018) 625–636, http://dx.doi.org/10.1016/j.snb.2017.12.132.
[41] S.A.M. Shaegh, A. Pourmand, M. Nabavinia, H. Avci, A. Tamayol, P. Mostafalu, H.B. Ghavifekr, E.N. Aghdam, M.R. Dokmeci, A. Khademhosseini, Rapid prototyping of whole-thermoplastic microfluidics with built-in microvalves using laser ablation and thermal fusion bonding, Sensors and Actuators B: Chemical. 255 (2018) 100–109, http://dx.doi.org/10.1016/j.snb.2017.07.138.
[42] D.J. Guckenberger, T.E. de Groot, A.M. Wan, D.J. Beebe, E.W. Young, Micromilling: a method for ultra-rapid prototyping of plastic microfluidic devices, Lab on a Chip. 15 (2015) 2364–2378, http://dx.doi.org/10.1039/C5LC00234F.
[43] H. Klank, J.P. Kutter, O. Geschke, CO 2-laser micromachining and back-end processing for rapid production of PMMA-based microfluidic systems, Lab on a Chip. 2 (2002) 242–246, http://dx.doi.org/10.1039/B206409J.
[44] M.V. Pergal, J. Nestorov, G. Tovilović, S. Ostojić, D. Gođevac, D. Vasiljević-Radović, J. Djonlagić, Structure and properties of thermoplastic polyurethanes based on poly (dimethylsiloxane): Assessment of biocompatibility, Journal of Biomedical Materials Research Part A. 102 (2014) 3951–3964, http://dx.doi.org/10.1002/jbm.a.35071.
[45] W.-I. Wu, K.N. Sask, J.L. Brash, P.R. Selvaganapathy, Polyurethane-based microfluidic devices for blood contacting applications, Lab on a Chip. 12 (2012) 960–970, http://dx.doi.org/10.1039/C2LC21075D.
[46] P. Gu, T. Nishida, Z.H. Fan, The use of polyurethane as an elastomer in thermoplastic microfluidic devices and the study of its creep properties, Electrophoresis. 35 (2014) 289–297, http://dx.doi.org/10.1002/elps.201300160.
[47] E. Piccin, W.K.T. Coltro, J.A.F. da Silva, S.C. Neto, L.H. Mazo, E. Carrilho, Polyurethane from biosource as a new material for fabrication of microfluidic devices by rapid prototyping, Journal of Chromatography A. 1173 (2007) 151–158, http://dx.doi.org/10.1016/j.chroma.2007.09.081.
[48] P.-C. Chen, C.-W. Pan, W.-C. Lee, K.-M. Li, An experimental study of micromilling parameters to manufacture microchannels on a PMMA substrate, The International Journal of Advanced Manufacturing Technology. 71 (2014) 1623–1630, http://dx.doi.org/10.1007/s00170-013-5555-z.
[49] I. Ogilvie, V. Sieben, C. Floquet, R. Zmijan, M. Mowlem, H. Morgan, Reduction of surface roughness for optical quality microfluidic devices in PMMA and COC, Journal of Micromechanics and Microengineering. 20 (2010), 065016, http://dx.doi.org/10.1088/0960-1317/20/6/065016.
[50] C.-W. Tsao, D.L. DeVoe, Bonding of thermoplastic polymer microfluidics, Microfluidics and Nanofluidics. 6 (2009) 1–16, http://dx.doi.org/10.1007/s10404-008-0361-x.
[51] S. Kumbar, C. Laurencin and M. Deng, Natural and synthetic biomedical polymers, ed., ed., Newnes, Vol. 2014.
[52] T. Ma, S. Sun, B. Li, J. Chu, Piezoelectric peristaltic micropump integrated on a microfluidic chip, Sensors and Actuators A: Physical. 292 (2019) 90–96, http://dx.doi.org/10.1016/j.sna.2019.04.005.
[53] Y. Zeng, M. Shin, T. Wang, Programmable active droplet generation enabled by integrated pneumatic micropumps, Lab on a Chip. 13 (2013) 267–273, http://dx.doi.org/10.1039/C2LC40906B.

Biographies

Amirhesam Banejad obtained a B.Sc. degree in 2016 from Bu-Ali Sina University, Hamedan, Iran, and a M.Sc. degree in 2019 from Ferdowsi University, Mashhad, Iran, both in Mechanical Engineering. His research included a design, fabrication and characterization of whole-thermoplastic microvalve and micropump with rectangular and half-elliptical cross-section. His research interests are the development of MEMS-based actuators, cancer diagnosis and microfluidics.

Mohammad Passandideh-Fard obtained a B.Sc. degree in 1987 from Ferdowsi University of Mashhad, Mashhad, Iran and a M.Sc. degree in 1989 from Isfahan University of Technology, Isfahan, Iran both in Mechanical Engineering. He earned his Ph.D. in Mechanical Engineering from the University of Toronto, Toronto, Canada in 1998. Dr. Passandideh-Fard has been a professor at the Department of Mechanical Engineering, Ferdowsi University of Mashhad from 2004. His research interests includes modeling and experimentation on free surface flows, nanofluidics for heat transfer enhancement purposes and microfluidics.

Hamidreza Niknam received the B.Sc. degree in Mechanical Engineering from Ferdowsi University of Mashhad in 2018. In 2018, he joined Bone & Joint Research Lab as a research assistant to work on thermoplastic-based microfluidic devices. He started his M.Sc. program from 2018 at Sharif University of Technology with focus on microchip-based methods for detection and separation of tumor cells. His research interests include development of microfluidics, cancer diagnosis and detection and separation of tumor cells.

Mohammad Javad Mirshojaeian Hosseini is a PhD student at School of Engineering Technology of Purdue Institute of Technology. Javad obtained his M.S. in Mechatronic Engineering (thesis: D̈esign, Simulation and Control of an Electro-Hydrostatic Actuator and Improvement of Its Performance¨) from K.N. Toosi University of Technology, Iran, and B.S. in Mechanical Engineering (thesis: Änalysis and examination of governing Equations of DC and AC Motors¨) from Ferdowsi University of Mashhad, Iran.

Seyed Ali Mousavi Shaegh received a B.S. and a M.S. in 2004 and 2007 from Yazd University, and Ferdowsi University of Mashhad, Iran, both in mechanical engineering. He received a Ph.D. in 2012 from Nanyang Technological University, Singapore, in Mechanical Engineering. He joined Harvard University, Brigham and Women's Hospital and Harvard-MIT Division of Health Sciences and Technology (HST), in 2014 as a postdoc fellow after a two-year research appointment at Singapore Institute of Manufacturing Technology (a research institute of Agency for Science, Technology and Research, A*STAR). Currently, he is an assistant professor of Biomedical Engineering at Mashhad University of Medical Sciences, in the School of Medicine (Clinical Research Unit and Orthopedic Research Center). Mousavi's research interests are mainly focused on microfluidic systems for diagnostics and drug testing, development of rapid prototyping methods for microfluidic chip fabrication, as well as design, fabrication, and testing of medical devices and implants.